

# Studies on Ferroelectric Poly(vinylidene fluoride) Langmuir-Blodgett Nanofilms Assisted by Polymer Nanosheets

著者	朱 慧娥
号	59
学位授与機関	Tohoku University
学位授与番号	工博第5013号
URL	<a href="http://hdl.handle.net/10097/62802">http://hdl.handle.net/10097/62802</a>

氏名 しゅ けいが  
 氏名 朱 慧娥  
 授与学位 博士 (工学)  
 学位授与年月日 平成26年9月24日  
 学位授与の根拠法規 学位規則第4条第1項  
 研究科, 専攻の名称 東北大学大学院工学研究科 (博士課程) 応用化学 専攻  
 学位論文題目 **Studies on Ferroelectric Poly(vinylidene fluoride) Langmuir–Blodgett Nanofilms Assisted by Polymer Nanosheets**  
 指導教員 東北大学教授 三ツ石 方也  
 論文審査委員 主査 東北大学教授 三ツ石 方也 東北大学教授 芥川 智行  
 東北大学教授 中川 勝

## 論文内容要旨

Poly(vinylidene fluoride) (PVDF) and its copolymers have attracted much attention because of their excellent mechanical and chemical properties, especially their interesting ferroelectric properties. Because of such special properties, their applications to superhydrophobic materials, nonvolatile low-voltage memories, nanogenerators, and even polymer bulk-heterojunction solar cells have been studied extensively. PVDF and its copolymers are semi-crystalline polymers, which have at least five phases:  $\alpha$ ,  $\beta$ ,  $\gamma$ ,  $\delta$ , and  $\varepsilon$  phases. Of all the phases, the all-trans polar  $\beta$  phase with the largest spontaneous polarization is responsible for its ferroelectricity. For practical applications, PVDF films at nanometer-scale-thick with high-content  $\beta$  phase are expected for low-voltage operation and high-density data storage. However, methods to obtain high content  $\beta$  phase in PVDF nanofilms are rarely reported to date because the crystallinity of PVDF films decreases markedly with the reduced film thickness. In this thesis, a facile method was described to versatile tuning of PVDF crystal forms from complete  $\alpha$  phase to complete  $\beta$  phase in PVDF Langmuir monolayers using different spreading solvents (**Chapter 2**). Preparation and properties of PVDF Langmuir–Blodgett (LB) nanofilms by assistance of a tiny amount of poly(*N*-dodecylacrylamide) (pDDA) (**Fig. 1**) were also demonstrated which show ultrahigh content of  $\beta$  crystals and adjustable film thickness by 2.3 nm per monolayer (**Chapter 3**). Finally, the application properties of as-prepared PVDF LB nanofilms were characterized with high remanent polarization ( $P_r$ ) values and a low fatigue rate (**Chapter 4**).

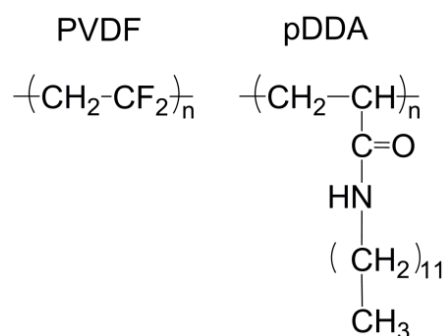


**Fig. 1** Chemical structures of PVDF and pDDA.

In our group, a polymer nanosheet of poly(*N*-dodecylacrylamide) (pDDA) (**Fig. 1**), has been built since 1987, which is an excellent amphiphilic polymer. The amide groups in pDDA backbone form well-organized hydrogen bonding network at the air–water interface, which makes the monolayer have unity transfer ratios onto various

substrates and available for preparing polymer nanosheets with monolayer thickness of about 1.7 nm. Taking advantage of the good film properties of pDDA monolayers, a plenty of functional polymer nanosheets have been

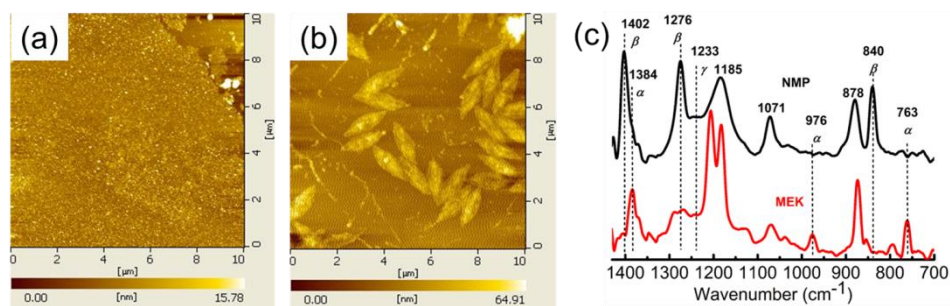


**Fig. 2** (a) FT-IR spectra of PVDF/pDDA LB nanofilms from NMP (black line) and MEK (red line), and AFM images of their LB monolayers (b) from NMP and (c) from MEK.

constructed, which are either copolymers of DDA and functional monomers or mixed pDDA/functional polymers with no amphiphilicity. Those nanosheets exert not only good film properties but also a variety of functionalities, which are applicable for photodevices, electrodevices, optical logic gates, or pH sensors. In Chapter 2, mixtures of ferroelectric poly(vinylidene fluoride) (PVDF) and amphiphilic pDDA were studied at the air–water interface for their monolayer behaviors. Using surface pressure ( $\pi$ )–area ( $A$ ) isotherms and Brewster angle microscopy (BAM) images, this study examined the formation of various pure PVDF and PVDF/pDDA Langmuir films. The spreading solvents play a key role in the properties of PVDF Langmuir films at the air–water interface, for instance *N*-methyl pyrrolidone (NMP) and methylethyl ketone (MEK). The PVDF(NMP) molecules at the air–water interface form scalable domains because of the high solubility of NMP in water. A miniscule amount of pDDA is effective in enhancing the properties of PVDF(NMP)/pDDA Langmuir films. The  $\pi$ – $A$  isotherms of PVDF(NMP) and pDDA mixtures at different molar ratios from 1:4 to 50:1 show a series of consecutive and steep curves with much higher collapse surface pressures ( $> 40$  mN/m) than that of pure PVDF (24 mN/m). This result is originated from the ordered hydrogen bonding network formed among pDDA molecules. Such a hydrogen bonding network is also the very reason that the transfer ability was enhanced tremendously in the PVDF(NMP)/pDDA Langmuir films. However, phase separation in PVDF(MEK)/pDDA Langmuir films was found from the two-plateau  $\pi$ – $A$  isotherms as well as the BAM images. This study provides valuable information related to the morphological evolution of semicrystalline PVDF confined in a pDDA two-dimensional geometry at the air–water interface and gives fundamental insight into the influence of solvents on the Langmuir film properties.

AFM images of PVDF(NMP)/pDDA and PVDF(MEK)/pDDA LB monolayers are respectively depicted in **Figs. 2a and b**. The PVDF(NMP)/pDDA LB monolayer has very smooth surface, however, the PVDF(MEK)/pDDA LB monolayer form regular diamond microstructures, analogous to the PVDF  $\alpha$ -single crystals. Well-known peaks at 763, 795, and 976  $\text{cm}^{-1}$  in FT-IR spectra are assigned to non-polar  $\alpha$  phase, and the  $\beta$  phase is associated with absorptions at 840, 1276, and 1402  $\text{cm}^{-1}$ . Then the peak at 1233  $\text{cm}^{-1}$  is characteristic for the  $\gamma$  phase. In the PVDF(NMP)/pDDA LB nanofilms(**Fig. 2c**), the peaks for  $\beta$  phase at 840, 1276, and 1402  $\text{cm}^{-1}$  are rather sharp, which are absent in the FTIR spectrum of PVDF(MEK)/pDDA LB nanofilms. In contrast, other peaks at 763 and 976  $\text{cm}^{-1}$  for  $\alpha$  phase and 1233  $\text{cm}^{-1}$  for  $\gamma$  phase are negligible in the PVDF(NMP)/pDDA LB nanofilms. Precise controlling of PVDF crystal structures in the nanofilms was realized. This study presents very interesting and controllable crystal structures in mixtures of nonamphiphilic PVDF and amphiphilic pDDA at the air–water

interface, which are expected to afford much useful information for additional interface manipulation of PVDF crystals.

The excellent property of monolayer formation was observed in PVDF(NMP)/pDDA Langmuir film (**Chapter 2**). In Chapter 3, studies were focused on the properties of PVDF(NMP)/pDDA LB multilayers vertically deposited from the water surface to substrates, which are promising for good organic ferroelectrics. This is the first report of the use of a vertical-dipping LB technique to acquire regular PVDF nanofilms. In the  $\pi$ -A isotherms of the mixed Langmuir films at the air-water interface, the rather high collapse surface pressure of PVDF quasi-monolayer at the mixing ratio of 50:1 is an important breakthrough in comparison with the reported values, which makes it successful to prepare highly dense PVDF LB nanofilms with a high film density, about  $1.82 \text{ g/cm}^3$  and a high crystallinity comparable to PVDF bulk, 52%. The absorption intensity at 196 nm from amide groups in pDDA molecules increases linearly along with the number of deposition layers (**Figs. 3a and b**), which indicates that these nanofilms have regular layer structures. The monolayer thickness was determined as 2.3 nm. The PVDF(NMP)/pDDA Langmuir film was deposited on one hydrophobic silicon substrate from 0 to 200 layers according to an arithmetic sequence with a common difference of 20 layers (**Fig. 3c**). The beautiful interference colors also prove the regular layer structure of the PVDF(NMP)/pDDA LB nanofilms, as well as the smooth film surface. In addition, the PVDF/pDDA LB nanofilms obtained with no post-treatment were demonstrated with dominant ferroelectric  $\beta$  phase (95 %) and negligible paraelectric  $\alpha$  phase by FT-IR spectra, as well as the XRD patterns. Furthermore, the high transfer properties, controllable  $\beta$ -crystal morphologies and film thickness and uniform film surface must endow the PVDF LB nanofilms with many applications as nanoelectronics such as high-performance memories, capacitors, transistors, and so on.

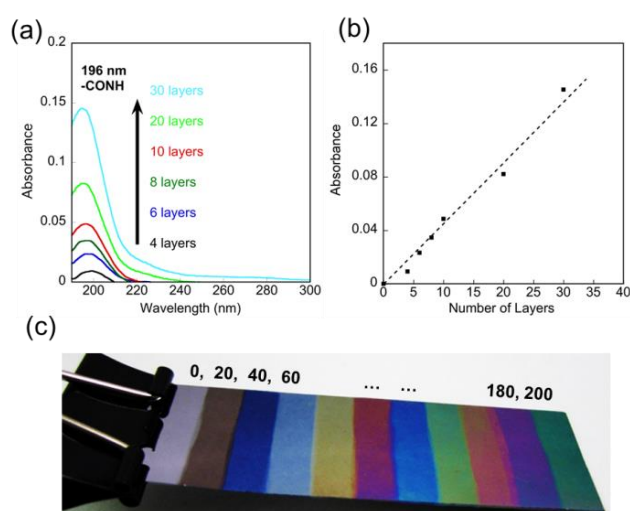


**Fig. 3** (a) UV-vis spectra of PVDF(NMP)/pDDA LB nanofilms (50:1), (b) relation between absorbance at 196 nm and number of layers, and (c) PVDF(NMP)/pDDA LB multilayers on a hydrophobic silicon substrate (from 0 to 200 layers).

The absorption intensity at 196 nm from amide groups in pDDA molecules increases linearly along with the number of deposition layers (**Figs. 3a and b**), which indicates that these nanofilms have regular layer structures. The monolayer thickness was determined as 2.3 nm. The PVDF(NMP)/pDDA Langmuir film was deposited on one hydrophobic silicon substrate from 0 to 200 layers according to an arithmetic sequence with a common difference of 20 layers (**Fig. 3c**). The beautiful interference colors also prove the regular layer structure of the PVDF(NMP)/pDDA LB nanofilms, as well as the smooth film surface. In addition, the PVDF/pDDA LB nanofilms obtained with no post-treatment were demonstrated with dominant ferroelectric  $\beta$  phase (95 %) and negligible paraelectric  $\alpha$  phase by FT-IR spectra, as well as the XRD patterns. Furthermore, the high transfer properties, controllable  $\beta$ -crystal morphologies and film thickness and uniform film surface must endow the PVDF LB nanofilms with many applications as nanoelectronics such as high-performance memories, capacitors, transistors, and so on.

In Chapter 4, ferroelectric nanocapacitors (FeNCs) made of as-deposited PVDF LB nanofilms (PVDF:pDDA = 50:1, from NMP) were fabricated with different film thicknesses of 12-81 nm by sandwiching the LB nanofilms between Al bottom and top electrodes. Ferroelectric polarization switching was investigated in the as-prepared PVDF FeNCs which show gradually saturated hysteresis loops with increasing film thickness (**Fig. 4a**). A remanent polarization ( $P_r$ ,  $E = 0$ ) value of  $6.6 \mu\text{C/cm}^2$  was obtained in 81-nm-thick PVDF LB nanofilms with no post-treatment such as thermal annealing. That value is one of the highest values ever reported for PVDF micro-/nanofilms. Such a high value must be attributed to the ultra-high content of  $\beta$  phase in these nanofilms. In addition, ferroelectricity was detected first in a PVDF homopolymer LB nanofilm as thin as 12 nm, indicating a potential low-voltage application of the nanofilms. The values of coercive electric field ( $E_c$ ,  $P_r = 0$ ) for the FeNCs in this study, approximately 195 MV/m are almost independent of the film thickness (**Fig. 4a**). Those values are

representative of the extrinsic switching characteristics of the PVDF LB nanofilms. The polarization switching process is dominated by inhomogeneous domain nucleation and growth. The breakdown strength of PVDF homopolymer LB nanofilms exceeds 500 MV/m (**Fig. 4a**). This value is much higher than that of bulk PVDF (about 300 MV/m). That fact indicates that PVDF LB nanofilms have good electric stability. The fatigue properties of the PVDF LB nanofilms provide useful information for elucidating the operation endurance of PVDF nanofilms thinner than 100 nm. All films from 12 to 81 nm showed long-standing fatigue endurance exceeding  $10^5$  cycles (**Fig. 4b**). In the case of the 81-nm thick PVDF homopolymer film,  $10^6$  cycle switching causes only 37 % loss of the  $P_r$  value. This is lower than that of a 69-nm thick P(VDF-TrFE) copolymer film. The  $P_r$  value reduces 50 % of its initial value under 150 MV/m, 1 kHz after  $10^6$  cycles. Therefore, the PVDF homopolymer LB nanofilms in this study occupy a lower fatigue rate than copolymers do.

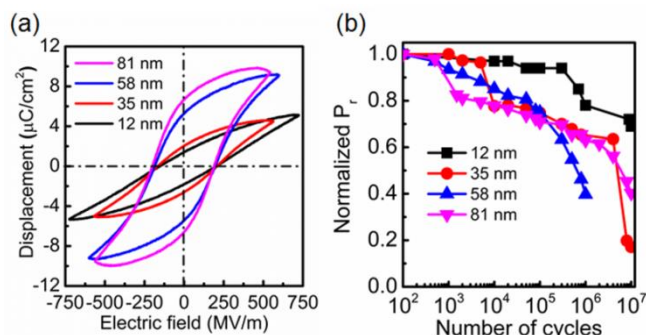


**Fig. 4** (a) Ferroelectric hysteresis loops and (b) Fatigue characteristics of ultrathin PVDF homopolymer LB nanofilms at different thicknesses.

In Chapter 5, I summarize the thesis. The monolayer behaviors of various PVDF Langmuir films were investigated using Brewster angle microscopy and surface pressure ( $\pi$ )–area (A) isotherms, which show significant dependence on spreading solvents. Thereafter, PVDF homopolymer Langmuir–Blodgett (LB) nanofilms were fabricated successfully by an assistance of amphiphilic pDDA nanosheets onto various substrates. The crystal structure of PVDF in the LB nanofilms is changeable from complete  $\alpha$  phase spread from MEK to complete  $\beta$  phase from NMP. In addition, the LB nanofilms show regular layer structures, high film density and high crystallinity with no post-treatment. The ferroelectricity of as-prepared PVDF LB nanofilms was observed with high remanent polarization ( $P_r$ ) value of  $6.6 \mu\text{C}/\text{cm}^2$  and high fatigue endurance exceeding  $10^5$  operation cycles. Therefore, the PVDF LB nanofilms are quite promising for non-volatile memory applications. All in all, the thesis proposed a systematic research to finely manipulate the properties of PVDF homopolymer nanofilms from monolayers to devices which have never been reported. It opens up many doors for further researches on ferroelectric polymer nanoelectronics aiming at practical applications. Not limited to ferroelectric polymers, the research results are also instructive and meaningful to crystallization controlling of other semi-crystalline polymers at the nano-scale with tunable film properties.

# 論文審査結果の要旨

ポリフッ化ビニリデン (PVDF) は高い機械的強度、耐薬品性を示し、強誘電性を示す興味深い高分子材料である。最近では、メモリデバイス、超撥水表面、ナノ発電への応用が報告されている。PVDF は様々な結晶相をとることが知られている。強誘電性を示すためには $\beta$ 相を示す必要があり、加熱・延伸などの処理がなされている。本論文では、強誘電性高分子 PVDF Langmuir-Blodgett(LB)ナノ薄膜の作製、およびそのナノエレクトロニクスデバイスへの応用について検討した研究の成果をまとめたものであり、全編 5 章より構成されている。

第 1 章は緒言であり、本研究の背景と目的について述べている。

第 2 章では PVDF LB ナノ薄膜を得るための水面上での単分子膜挙動について検討を行っている。PVDF を *N*-メチルピロリドン (NMP) に溶解し、ポリ(*N*-ドデシルアクリルアミド) (pDDA) のクロロホルム溶液と別々に Langmuir トラフ上に展開し、様々な混合比で表面圧( $\pi$ )一面積(A)等温線を測定したところ、PVDF:pDDA=50:1 の場合でも高い崩壊圧を有する $\pi$ -A 等温線が得られることを見出した。PVDF 単体では高い崩壊圧を得ることはできず、pDDA が PVDF の水面上での超薄膜化を可能としていることを示唆する。PVDF をメチルエチルケトン (MEK) に溶解した場合、混合比に応じて、 $\pi$ -A 等温線は 2 つの平坦部を示した。水面上で PVDF と pDDA が相分離していることを意味する。これらの様子は Brewster 角顕微鏡観察により確認された。興味深いことに固体基板上に転写されたそれぞれの PVDF LB ナノ薄膜は、NMP では $\beta$ 相、MEK では $\alpha$ 相が高效率で形成されていることを FTIR や原子間力顕微鏡により明らかにしている。

第 3 章では、第 2 章で見出した NMP を用いた PVDF LB ナノ薄膜の膜構造と累積特性について検討を行った。固体基板を垂直浸漬することで、累積比ほぼ 1 で水面上の PVDF 超薄膜を転写することができた。混合比が高くなると、膜中にファイバー状の PVDF が見られるようになり、その膜厚は 1 層あたり約 2.3 nm と求められた。この手法により 200 層まで規則正しく累積が可能であり、 $\beta$ 相の割合が 95% と非常に高い割合であること、熱処理を行わなくとも高效率の $\beta$ 相を含む PVDF LB ナノ薄膜を得られることを UV 吸収スペクトル、X 線回折、FTIR などを用いて明らかにした。

第 4 章では、PVDF LB ナノ薄膜の強誘電性について評価を行った。ケルビンプローブフォース顕微鏡を用いて、PVDF ナノ薄膜を観察した。膜厚 12nm の PVDF LB ナノ薄膜を用いて、あらかじめ分極した部分のみが異なる表面電位を有する像として画像化することに成功した。Al を電極としたサンドイッチ型の PVDF ナノ薄膜のキャパシタを作製し、自作の装置を用いて Sawyer-Tower 法により PVDF ナノ薄膜の残留分極を測定したところ、膜厚 81 nm のキャパシタについて 6.6 mm/cm<sup>2</sup> の値を得た。この値はホモポリマー PVDF の超薄膜としては非常に大きな値である。また、残留分極は 10<sup>6</sup> サイクル後も 37% の減少に抑えることができ、PVDF LB ナノ薄膜の優れた強誘電性特性を明らかにした。

第 5 章は本論文の総括である。

以上要するに本論文は、気水界面を利用する Langmuir-Blodgett 法と高分子ナノシートにより強誘電性高分子 PVDF のナノ構造を制御し、強誘電性を示す $\beta$ 相を高效率に含む PVDF LB ナノ薄膜を作製する技術を見出し、その結晶構造制御に関する実験的指針および強誘電性に由来したキャパシタ特性に関する基礎的性質を明らかにした。PVDF LB ナノ薄膜が、これまで得られていない膜厚 100nm 以下での高い繰り返し特性という新しい領域の材料であること、さらには強誘電性高分子超薄膜作製技術が様々な結晶性高分子やナノ材料への拡張可能であることを示した研究であり、高分子化学及び材料化学の発展に寄与するところが少なくない。

よって、本論文は博士(工学)の学位論文として合格と認める。